ELSEVIER

Ceramics International 33 (2007) 979–985

CERAMICS INTERNATIONAL

www.elsevier.com/locate/ceramint

Properties of β-$Ca_3(PO_4)_2$ bioceramics prepared using nano-size powders

Kaili Lin, Jiang Chang *, Jianxi Lu, Wei Wu, Yi Zeng

Shanghai Institute of Ceramics, Chinese Academy of Sciences, 1295 Dingxi Road, Shanghai 200050, P.R. China

Received 7 July 2005; received in revised form 3 January 2006; accepted 27 February 2006
Available online 18 April 2006

Abstract

Nano-size β-TCP powders with average grain size of 100 nm were prepared by the precipitation method. The sinterability of the nano-size powders, and the microstructure, mechanical strength and the in vitro degradability of the prepared β-TCP bioceramics were investigated. The results showed that the nano-size powders possessed superior sintering properties as compared to the micro-size powders. The densification temperature and phase transition temperature of β-TCP bioceramics prepared using nano-size powders was clearly lower than that prepared using micro-size powders, and the maximum value of the bending strength, elastic modulus, Vickers hardness and compressive strength of the samples fabricated from nano-size powders were more than two-times higher as compared to those of samples fabricated from micro-size powders. Furthermore, the degradability of the β-TCP bioceramics fabricated from nano-size powders was much lower than for micro-size powders, suggesting the possible control of the degradability of the bioceramics by regulating powder size.

Keywords: A. Sintering; C. Mechanical Properties; β-Tricalcium phosphate; Nano-size; Micro-size; Degradability

1. Introduction

β-TCP has been proved to be resorbable in vivo with new bone growth replacing the implanted β-TCP [1–3]. This property imparts significant advantage onto β-TCP compared to other biomedical materials, which are not resorbed and replaced by natural bone. Therefore, β-TCP bioceramics are widely used as bone replacements in the field of oral and plastic surgery [1,4–6].

Most of the β-TCP is implanted in the forms of granules and rods. It is well known that the low mechanical behaviour of β-TCP bioceramics is the main limitation in load-bearing applications in clinic [7,8]. Thus, despite their favorable biological properties, the poor mechanical strength of β-TCP bioceramics has severely hindered their clinical applications [7,8]. For many years, a number of studies have been focused on the sintering properties of β-TCP bioceramics, aiming at improving their mechanical strength [9,10], and studies have shown that the mechanical strength of the ceramics is a function of density, grain size, grain morphology and grain boundary characteristics [11–14]. Low temperature sintering is an effective way to obtain high mechanical strength of ceramics by avoiding grain size growing excessively and obtaining high-density bodies with fine grain size. However, the sintering activity of the widely used commercial β-TCP powders with micro- or submicro-size was poor, and high sintering temperature (commonly $>1150\ ^{\circ}C$) is required to obtain high-density β-TCP matrix with large grain sizes [10,15,16]. It is known that nano-size ceramic powders have high surface area and high sintering activity, which may result in the high mechanical strength of fully dense matrix with fine grain size at low sintering temperature [17].

However, up to now, most work was focused on the parameters which would influence the β-TCP powder characteristics [18–20], few work has been carried out on the sintering behavior of the powders with different particle size, and their influences on the properties of the sintered β-TCP matrix. The aim of the present study was to investigate the influence of the nano-size powders and commercially obtained micro-size powders on the sintering, microstructure, mechanical strength and degradability of the β-TCP bioceramics.

* Corresponding author. Tel.: +86 21 52412804; fax: +86 21 52413903.
E-mail address: jchang@mail.sic.ac.cn (J. Chang).

0272-8842/$32.00
doi:10.1016/j.ceramint.2006.02.011

2. Materials and methods

2.1. Materials

The micro-size β-TCP powders were obtained from Tomita (Tokushima, Japan) and the grain size of the powders is in the range of 0.5–3 μm. All other chemicals were obtained from China National Medicine Shanghai Chemical Reagent Corporation.

2.2. Preparation of nano-size β-TCP powders

The nano-size β-TCP powders for the present studies were synthesized by the reaction of $Ca(NO_3)_2$ with $(NH_4)_2HPO_4$. Briefly, 1000 mL of 0.4 mol $(NH_4)_2HPO_4$ solution with a pH 10.8 was vigorously stirred at room temperature, and 1000 mL of 0.6 mol $Ca(NO_3)_2$ with a pH 10.8 was added dropwise over 300–360 min to produce a white precipitate. Throughout the mixing process the pH of the system was maintained above 10.8 with the adding of ammonia solution. The white precipitate was then stirred for 12 h followed by washing with distilled water, and then washed with 100% ethanol to improve the dispersion characteristics. After washing, the remaining liquid was removed by vacuum filtration, and the precipitate was dried at 80 °C for 24 h. β-TCP was obtained by calcining the powders at 800 °C for 2 h.

2.3. Preparation of β-TCP bioceramics

The prepared nano-size β-TCP powders and the commercially obtained micro-size β-TCP powders were used as the starting raw materials. The powders were uniaxially pressed and followed by cold isostatic pressing into rectangular-prism-shaped specimens (≈44 mm × 8 mm × 4 mm) under a pressure of 200 MPa for 15 min. Subsequently, they were pressurelessly sintered in air at selected temperatures for 2 h with a heating rate of 3 °C/min. The samples were cooled to room temperature at a rate of 2 °C/min in the furnace.

2.4. Characterization of β-TCP powders and bioceramics

The morphology and size of the synthesized and commercially obtained β-TCP powders were observed by transmission electron microscopy (TEM: JEM-2100F, JEOL, Japan). XRD patterns of the β-TCP powders and ceramics were characterized by X-ray diffraction (XRD: D/max 2550 V, Rigaku, Japan). The chemical composition of the synthesized and commercial β-TCP powders was analyzed by inductively coupled plasma atomic emission spectroscopy (ICP-AES; VISTA AX, Varian Co., USA). The open porosity and relative densities of the sintered samples were determined by the Archimedian method [21] with distilled water as the immersion medium, and the closed porosity was calculated using the bulk and real density of the samples [22]. The sintered samples were mirror-polished using 0.5 μm diamond slurries. After polishing and etching at 100 °C below the sintering temperature for 1 h, the surface of the sintered samples was observed by field emission scanning electron microscope (FESEM: JSE-6700F, JEOL, Japan). The three-point bending strength and elastic modulus of the sintered samples were measured at the mechanical testing machine (Shimadza AG-5 kN, Japan) with a loading rate of 0.5 mm/min according to the JIS R1601 and JIS R1602 standard, respectively. A span length of 30 mm and rectangular-prism-shaped specimens (36 mm × 4 mm × 3 mm) with surfaces polished by 0.5 mm diamond powders were used. The Vickers hardness of the samples was measured on the polished surface using a load of 1 kg and 10 s of indentation time (Wilson-wolpert Tulkon® 2100B, Instron, USA) according to the ISO 14705-2002 standard. The compressive strength of the sintered samples in the size of 6 mm × 6 mm × 3 mm was measured using a mechanical testing machine (5500R-100 kN, Instron, USA) with a loading rate of 0.5 mm/min according to the GB/T 8489-1987 standard. In this study, five samples from each group were tested to obtain average relative density, bending strength, elastic modulus, Vickers hardness and compressive strength.

2.5. Soaking in Tris–HCl buffer solution

The degradability of the fabricated β-TCP bioceramics was determined by their weight loss percentage in Tris–HCl buffer solution. The 0.1 M Tris–HCl buffer solution was prepared by dissolving analytical reagent grade Tris(hydroxymethyl) aminomethane in distilled water and then was buffered at pH 7.4 at 37 °C with hydrochloric acid. The sintered β-TCP bioceramics were placed in polystyrene bottles containing Tris–HCl buffer solution. The bottles with the samples and Tris–HCl were maintained at 37.0 °C in a shaking water bath for 1, 3, 7,14, 21 and 28 days, respectively, for the degradation experiment, at the ratio of surface area (cm^2) to solution volume (mL) of 0.1 and refreshing the soaking medium every 24 h. After various soaking periods, the samples were took out and rinsed with deionized water followed by drying in vacuum at 150 °C before further characterization. In this study, three samples from each group were tested to obtain an average degradability.

3. Results

The morphology and size of the prepared and the commercial β-TCP powders are shown in Fig. 1. It is clear to see that the two powders possessed quite distinctive characteristics in shape, size and size distribution. The prepared β-TCP powders (Fig. 1A) showed less agglomerative morphologies and uniform particle size. The average particle size was about 100 nm, while the commercially obtained β-TCP powders (Fig. 1B) showed agglomerative morphologies and irregular particle shapes. The powder size distribution was in the wide range of between 0.5 μm and 3 μm.

Fig. 2 shows the XRD patterns of the as-prepared powders. The results revealed that the as-prepared powders were composed of highly crystalline and no second phase other than β-TCP.

Table 1 shows the chemical composition of the prepared nano-size and the commercial micro-size β-TCP powders. It is

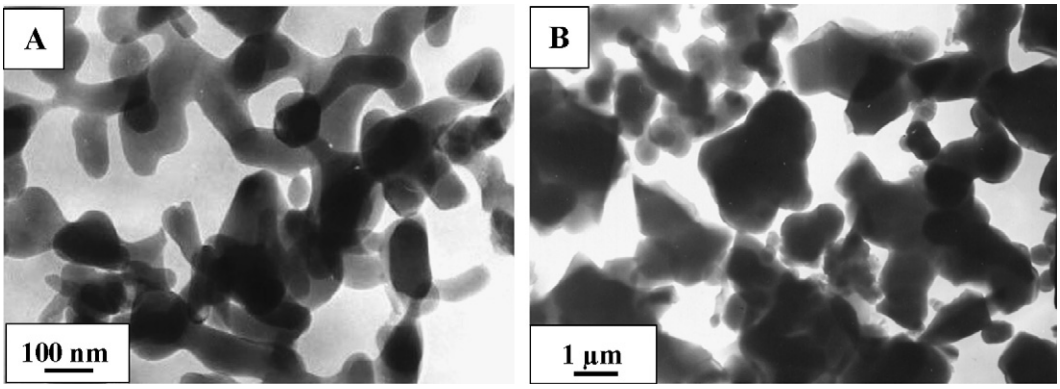

Fig. 1. TEM micrograph of the β-TCP powders: as-prepared nano-size powders (A); commercial micro-size powders (B).

clear to see that the impurity chemical composition of Mg and Fe in the commercial micro-size β-TCP powders was much higher than those in the prepared nano-size powders. The Ca/P molar ratio of the prepared nano-size powders equal to the theoretic value of 1.50. However, the Ca/P molar ratio of the commercial micro-size powders only reached 1.47, which was slightly lower than theoretic value of 1.50.

Fig. 3 shows the relative densities (RD) of the samples sintered from nano-size powders and micro-size powders as a function of the sintering temperature. Density could be seen to increase with increasing sintering temperature. When sintered at 950 °C, the RD of the ceramics fabricated from commercial β-TCP powders only reached 64.29%. With the increase of the sintering temperature to 1000 °C, the relative density increased slowly to 66.11%. Further increase the temperatures, the RD increased sharply, and reached 95.66% at 1160 °C. As expected, the nano-size powders reached a fairly high density (93.81% RD) even sintered at a temperature as low as 950 °C. When the sintering temperature increased to 1000 °C, the sintered specimen almost reached its theoretical density (97.72% RD), which was much denser than those fabricated from the micro-size powders. By further increasing the sintering temperature to 1100 °C, it reached fully dense (99.54% RD). When the sintering temperature increased to 1160 °C, the RD decreased to 94.95%. This phenomenon was attributed to the transformation of β-TCP to α-TCP (validated by XRD in Fig. 4).

Table 1
The chemical content of the prepared and the commercial β-TCP powders

Element content (wt.%)	Ca	P	Mg	Fe	Ca/P molar ratio
Commerical powders	39.41	20.72	0.059	0.0016	1.47
Prepared powders	39.52	20.36	0.0003	0.0002	1.50

Fig. 4 shows the XRD patterns of the samples sintered from the nano-size and micro-size β-TCP powders, respectively. It can be seen that the samples fabricated from nano-size powders and sintered at 1100 °C were composed of highly crystalline and single-phase β-TCP, and no other phases were observed. When the sintering temperature increased to 1160 °C, β-TCP was completely transformed to α-TCP. In contrast, the β-TCP ceramics fabricated from micro-size powders were maintained in β-phase even sintered at 1160 °C and no peaks of α-TCP could not be observed.

The microstructural observations also revealed significant differences between β-TCP bioceramics fabricated using different powders (Fig. 5). The samples fabricated from nano-size powders had highly densified bodies, which was in agreement with the relative density values. The grain shapes

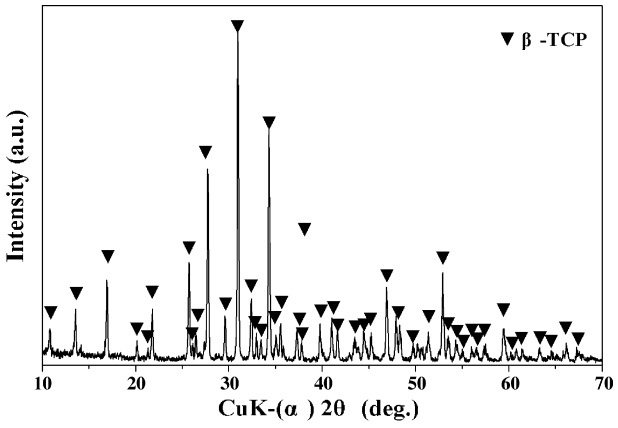

Fig. 2. XRD patterns of the as-prepared β-TCP powders.

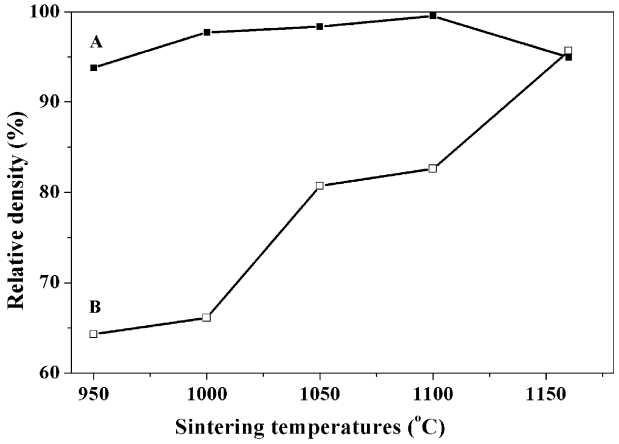

Fig. 3. Relative density of β-TCP bioceramics fabricated from nano-size powders (A) and micro-size powders (B).

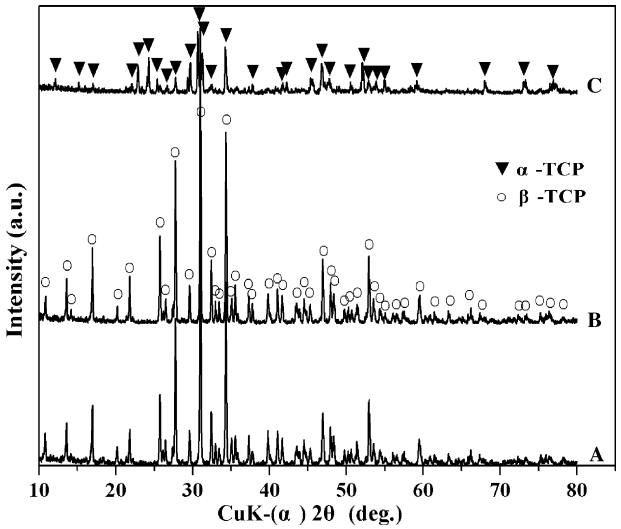

Fig. 4. XRD patterns of β-TCP bioceramics prepared using nano-size and micro-size powders: (A) nano-size powders sintered at 1100 °C, (B) commercial micro-size powders sintered at 1160 °C, and (C) nano-size powders sintered at 1160 °C.

were uniform and the average grain size was about 0.3 μm. On the contrary, the samples fabricated from commercial micro-size powders showed much coarser and tortuous surface morphology with 0.3–0.5 μm intergranular pores in the matrix, and the average grain size was approximately 5 μm. Table 2 shows the open porosity, closed porosity and the open versus close porosity of the samples sintered from different β-TCP powders. It is clear to see that the open porosity of the samples fabricated from the commercially obtained powders and the prepared powders was 4.38% and 0.48%, respectively, and the closed porosity of the samples was 2.98% and 0.13%, respectively. The open versus close porosity of the samples sintered from the micro-size powders and nano-size powders reached about 1.5:1 and 3.7:1, respectively. The distinct characteristic of the microstructure and porosity of the samples fabricated from different powders might result in quite different mechanical strength and other properties.

Table 3 shows the mechanical strength of the β-TCP bioceramics sintered from nano-size and micro-size powders at 1100 °C and 1160 °C, respectively. It is clear to see that the

Table 2
The open porosity, closed porosity and the open versus close porosity of the samples sintered from different β-TCP powders

Samples	Open porosity (%)	Closed porosity (%)	Open versus close porosity
Fabricated from micro-size powders	4.38 ± 0.52	2.98 ± 0.26	1.5:1
Fabricated from nano-size powders	0.48 ± 0.06	0.13 ± 0.04	3.7:1

mechanical strength of the samples fabricated from nano-size powders were much higher than those fabricated from micro-size powders. The maximal value of the bending strength, elastic module, Vickers hardness and compressive strength of the samples fabricated from nano-size β-TCP powders were more than two-times higher as compared to those of bioceramics obtained from commercial micro-size β-TCP powders. The bending strength of the β-TCP bioceramics fabricated by nano-size powders was about 200 MPa, much higher than the data reported in the literatures for β-TCP bioceramics [2,15]. Furthermore, for the samples fabricated from micro-size β-TCP powders, an increase of the sintering temperature from 1100 °C to 1160 °C resulted in the increase of the mechanical strength, which was due to the improved density at higher sintering temperature. In contrast, the mechanical properties (bending strength, compressive strength, elastic modules and hardness) of the ceramics prepared from nano-size β-TCP powders decreased obviously with the increase of the sintering temperature form 1100 °C to 1160 °C, which was caused by the phase transformation and accompanied decrease in the density of the sintered bodies.

Fig. 6 shows the degradability (weight loss percentage, wt.%) of the β-TCP bioceramics fabricated from nano-size and micro-size powders and sintered at 1100 °C and 1160 °C, respectively in Tris–HCl buffer solution. Degradability can be seen to increase with increasing soaking time. It is clear to see that the degradation of the samples sintered from nano-size powders only reached 0.09% at day 1. With the soaking time increasing, the degradation increased slowly, and reached 0.44% at day 14 and then increased step by step and reached 1.62% at day 28. In contrast, the degradation of the samples

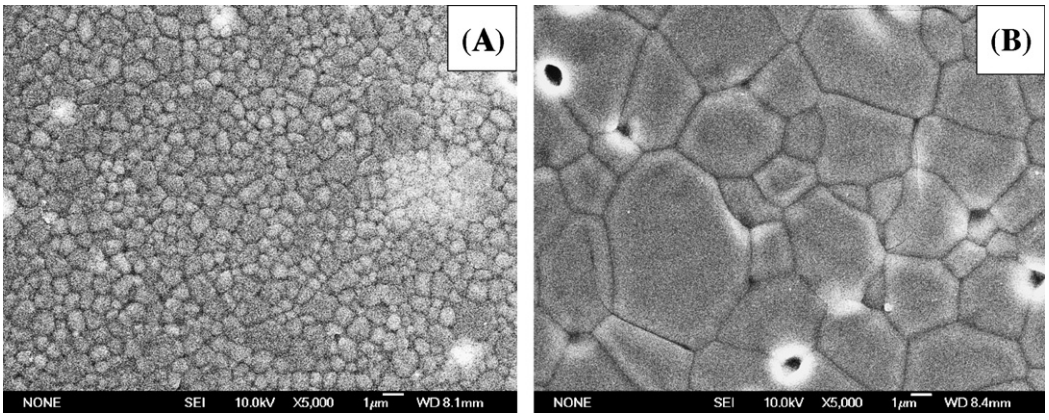

Fig. 5. FESEM micrograph of β-TCP bioceramics fabricated from nano-size powders at 1100 °C (A) and micro-size powders at 1160 °C (B).

Table 3
Mechanical strength of the samples fabricated from nano-size and micro-size β-TCP powders

Samples	Bending strength (MPa)	Elastic module (GPa)	Vickers hardness (H_V)	Compressive strength (MPa)
Nano-size powders sintered at 1100 °C	198.85 ± 4.61	69.49 ± 3.51	529 ± 12	573.99 ± 25.14
Micro-size powders sintered at 1100 °C	61.45 ± 1.98	24.93 ± 2.17	198 ± 25	218.59 ± 15.62
Nano-size powders sintered at 1160 °C	125.12 ± 3.79	41.43 ± 2.62	288 ± 31	391.32 ± 29.15
Micro-size powders sintered at 1160 °C	81.45 ± 2.12	34.43 ± 1.45	269 ± 36	278.93 ± 15.95

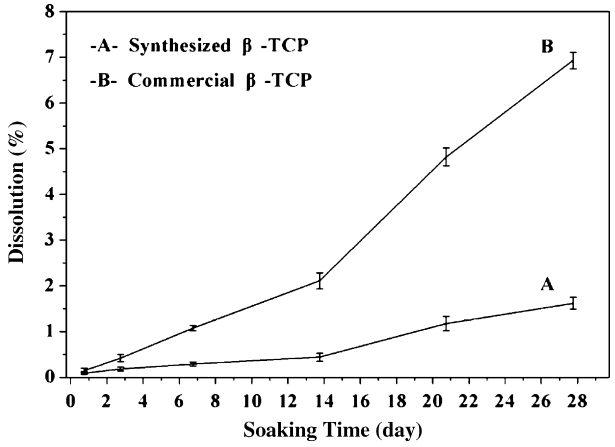

Fig. 6. Degradability of the β-TCP bioceramics sintered from nano-size powders at 1100 °C (A) and micro-size powders at 1160 °C (B).

fabricated from micro-size powders was much faster than those fabricated from nano-size powders. At day 1, it reached 0.15%. With the increase of the soaking time, the degradation increased sharply, and reached 6.93% at day 28. The results show that the extent of degradation is approximately four-times higher for the samples fabricated from micro-size powders compared to that for the nano-size powders.

4. Discussion

The present study has demonstrated that the distinct influence of nano-size and micro-size β-TCP powders on the sintering ability, microstructure, mechanical strength and degradability of the β-TCP bioceramics. The precipitation prepared nano-size β-TCP powders showed less agglomerative morphologies and uniform particle size with average particle size of 100 nm, while the commercial micro-size β-TCP powders showed agglomerative morphologies and irregular particle shapes, and the powder size distribution was in the wide range between 0.5 μm and 3 μm. The purity of the prepared nano-size β-TCP powders was much higher than that of commercial micro-size β-TCP powders. The distinct characteristic of these nano-size β-TCP powders and micro-size β-TCP powders resulted in quite different sintering ability and other properties.

The densification curves obtained from nano-size powders and micro-size powders indicated that employing nano-size powders effectively lowered the densification temperature by several 100 °C, which indicates a high sintering efficiency using nano-size powders, and suggests that using nano-size β-TCP powders was an available method for fabricating highly densified β-TCP bioceramics at lower sintering temperature. The difference in sintering behavior is directly related to the initial particle size and shape of the powders. Previous studies have shown that, as compared to the micro-size powders, the nano-size powders with uniform grain size and less agglomeration have much higher driving force for densification due to the enormous surface area [23]. In the processes of ceramic sintering, as the sintering temperature increased, the driving force for densification and the rate of grain boundary motion increases, and breakaway of the boundaries from the pores and leaving of isolated pores in the grain interior occurs because the pores are slower moving than the grain boundaries [24]. Under the tension of a moving grain boundary, pores can move by volume or surface diffusion or even by evaporation–condensation across the pores [25]. In contrast, the pores in the ceramics fabricated from micro-size powders with irregular grain size cannot be completely removed by rapid sintering rate and remain as closed pores which limits the final densification [25]. On the other hand, the wide particle size distribution of the micro-size powders with agglomerates and irregular morphology causes poor packing, which can also cause the exaggerated grain growth during sintering.

The microstructural difference was in agreement with the relative density values shown in Fig. 3. The remarkable difference of the sintering ability of the nano-size and micro-size β-TCP powders resulted in the significant differences of the relative density and microstructure of the sintered matrixes, and clearly affected the mechanical properties of the sintered matrixes [11]. Based on the previous studies [12–14], the bending strength, elastic module, Vickers hardness and compressive strength of the ceramics increase as the density increasing and grain size decreasing. Our results showed that employing nano-size β-TCP powders as raw materials could effectively increase the sintering density, avoiding the excessive growing of the grain size, obtaining fully dense and microstructural homogeneities of the β-TCP matrix with fine grain size, and leading to higher mechanical strength at a relative lower sintering temperature.

It is interesting to see that the phase transition from β- to α-TCP appeared to happen at lower temperature for the ceramics prepared from nano-size β-TCP powders than for that from commercially obtained micro-size β-TCP powders. The previous studies have shown that the residual Mg and/or Fe content in β-TCP powders could substantially raise the phase transition temperature from β- to α-TCP of the β-TCP ceramics

[26–28]. The residual Mg and Fe content in the commercial micro-size β-TCP powders were much higher than that in the prepared nano-size β-TCP powders. Therefore, the phase transition from β- to α-TCP appeared to happen at higher temperature for the ceramics prepared from commercially obtained micro-size β-TCP powders than for that from prepared nano-size β-TCP powders.

The degradability of β-TCP bioceramics is an important property, which plays a key role for its application as bone repair materials. The degradability rate of the β-TCP bioceramics is determined by many factors, such as sintering parameters, microstructure, porosity and crystallinity of the ceramics. Factors tending to increase degradation rate include the increase in porosity and the increase in number of crystal imperfections [29–31], and the porosity plays a dominant role in degradation of ceramics [31]. The in vivo studies have also confirmed that the degradation rate of the sintered calcium phosphate bioceramcis increases with the increase of the porosities [31–33]. Previous studies suggested that the degradation mechanism of the Ca-P bioceramics sintered at a high temperature with good crystallization is mainly the solution dissolution, and the dissolution always happen easily on the boundary of the open micro-pores [30,31]. The different sintering ability of the prepared nano-size β-TCP powders and the commercially obtained micro-size β-TCP powders resulted in the different microstructures of the sintered matrixes. The ceramic samples fabricated from nano-size β-TCP powders and sintering at 1100 °C reached fully dense (99.54%), and the open porosity and the closed porosity only reached 0.48% and 0.13%, respectively. However, the relative density of the samples fabricated from the micro-size β-TCP powders and sintered at 1160 °C only reached 95.66%, and the open and closed porosity reached 4.38% and 2.98%, respectively. The open porosity of the samples fabricated from the micro-size β-TCP powders was much higher than those samples fabricated from nano-size β-TCP powders. Therefore, the degradation rate of the samples derived from micro-size powders was much faster than those derived from nano-size powders. The dissolution increased slowly within 14 days with the increase of the soaking time. In contrast, the dissolution of the samples fabricated from micro-size powders increased much faster than those fabricated from nano-size powders after 14 days, which might be attributed to the closed pores, which were opened gradually by the dissolution. In fact, the degradation mechanisms of the Ca-P based bioceramics in vitro are very complex, including the dissolution, hydrolyzation and ion adsorption, etc. [26,34]. The relative significance of these mechanisms is not yet clear, and the factors concerning the degradation of the Ca-P based bioceramics have not been completely elucidated [35]. The chemical composition, physical characteristics and crystal structures certainly play an important role in the degradation mechanisms [36–38]. Numerous studies have confirmed that Ca-P based ceramics can be dissolved in vitro [30,39] and in vivo [29,39,40]. However, the dissolution processes of the β-TCP bioceramics in vivo and in vitro need to be further investigated in detail, and are under study.

5. Conclusions

The sintering ability of the nano-size β-TCP powders, and the microstructure, mechanical strength and the in vitro degradability of the prepared β-TCP bioceramics were investigated. The results showed that the sintering ability of the nano-size β-TCP powders was much higher than the micro-size β-TCP powders. Using nano-size β-TCP powders as raw materials is an effective way to obtain dense ceramics with high mechanical strength and fine grain size at low sintering temperature. The maximal value of the bending strength, elastic module, Vickers hardness and compressive strength of the samples fabricated from nano-size β-TCP powders were more than two-times higher as compared to those of bioceramics obtained from micro-size β-TCP powders. Furthermore, the degradability of the bioceramics sintered from nano-size powders was just about one fourth of those from micro-size powders, which indicated that the degradability of β-TCP bioceramics also could be regulated by the powder size.

Acknowledgments

This work was supported by grants from Science and Technology Commission of Shanghai Municipality (Grant No.: 0352nm119, 047252043, 05DJ14005), and the National Basic Research Program (<9 7 3> Program) of P.R. China (Grant No.: 2005CB522704).

References

[1] R.Z. LeGeros, J.P. LeGeros, in: L.L. Hench, J. Wilson (Eds.), An Introduction to Ceramics, World Scientific, Singapore, 1993.
[2] L.L. Hench, Bioceramics, J. Am. Ceram. Soc. 81 (7) (1998) 1705–1728.
[3] B.V. Rejda, J.G.J. Peelen, K. de Groot, Tricalcium phosphate as a bone substitute, J. Bioeng. 1 (2) (1997) 93–96.
[4] K. de Groot, Clinical applications of calcium phosphate biomaterials: a review, Ceram. Int. 19 (5) (1993) 363–366.
[5] S. Qu, W. Chen, J. Weng, X. Zhang, in: Y. Urpo, H. Anderson (Eds.), Bioceramics, 7, Butterworth-Heinemann, London, 1994, p. 91.
[6] C. Lavernia, J. Schoenung, Calcium phosphate ceramics as bone substitutes, Ceram. Bull. 70 (1) (1991) 95–100.
[7] P. Ducheyne, Bioceramics: material characteristic versus in vivo behavior, J. Biomed. Mater. Res. 21 (2) (1987) 219–236.
[8] M.J. Yaszemski, R.G. Payne, W.C. Hayes, R. Lander, A.G. Mikos, Evolution of bone transplantation: molecular, cellular and tissue strategies to engineer human bone, Biomaterials 17 (2) (1996) 175–185.
[9] M. Jarcho, R.L. Salisbury, M.B. Thomas, R.H. Doremus, Synthesis and fabrication of β-tricalcium phosphate ceramics for potential prosthetic application, J. Mater. Sci. 14 (1) (1979) 142–150.
[10] A. Tampieri, G. Celotti, F. Szontagh, E. Landi, Sintering and characterization of HA and TCP bioceramics with control of their strength and phase purity, J. Mater. Sci.: Mater. Med. 8 (1) (1997) 29–37.
[11] N. Thangamani, K. Chinnakali, F.D. Gnanam, The effect of powder processing on densification, microstructure and mechanical properties of hydroxyapatite, Ceram. Int. 28 (4) (2002) 355–362.
[12] N.J. Petch, The cleavage strength of polycrystals, J. Iron Steel Inst. 174 (1) (1953) 25–28.
[13] F.P. Knudsen, Dependence of mechanical strength of brittle polycrystalline specimens on porosity and grain size, J. Am. Ceram. Soc. 42 (8) (1959) 376–387.

[14] R.W. Rice, Comparison of stress concentration versus minimum solid area based mechanical property—porosity relations, J. Mater. Sci. 28 (8) (1993) 2187–2190.
[15] M. Akao, H. Aoki, K. Kato, A. Sato, Dense polycrystalline β-tricalcium phosphate for prosthetic applications, J. Mater. Sci. 17 (2) (1982) 343–346.
[16] H.K. Varma, S. Sureshbabu, Oriented growth of surface grains in sintered β-tricalcium phosphate bioceramics, Mater. Lett. 49 (2) (2001) 83–85.
[17] K.C.B. Yeong, J. Wang, S.C. Ng, Fabricating densified hydroxyapatite ceramics from a precipitated precursor, Mater. Lett. 38 (3) (1999) 208–213.
[18] A. Destainville, E. Champion, D. Bernache-Assollant, E. Laborde, Synthesis, characterization and thermal behavior of apatitic tricalcium phosphate, Mater. Chem. Phys. 80 (1) (2003) 269–277.
[19] I. Manjubala, M. Sivakumar, In-situ synthesis of biphasic calcium phosphate ceramics using microwave irradiation, Mater. Chem. Phys. 71 (3) (2001) 272–278.
[20] J.S. Bow, S.C. Liou, S.Y. Chen, Structural characterization of room-temperature synthesized nano-sized β-tricalcium phosphate, Biomaterials 25 (16) (2004) 3155–3161.
[21] N.O. Engin, A.C. Tas, Manufacture of macroporous calcium hydroxyapatite bioceramics, J. Eur. Ceram. Soc. 19 (13–14) (1999) 2569–2572.
[22] R.S. Byrne, P.B. Deasy, Use of commercial porous ceramic particles for sustained drug delivery, Int. J. Pharm. 246 (1–2) (2002) 61–73.
[23] A.S. Edelstein, R.C. Cammarata (Eds.), Nanomaterials: Synthesis, Properties and Applications, Institute of Physics (IOP), Bristol, England, 1996.
[24] R.J. Brook, Pore and grain growth kinetics, J. Am. Ceram. Soc. 52 (6) (1969) 339–340.
[25] D.W. Richerson (Ed.), Modern Ceramic Engineering: Properties, Processing and Use in Design, Marcel Dekker, New York, 1922.
[26] J.C. Elliott, Structure and Chemistry of the Apatites and Other Calcium Orthophosphates, Elsevier, Amsterdam, 1994.
[27] R. Famery, P.B. Richard, Preparation of α- and β-TCP ceramics, with and without magnesium addition, Ceram. Int. 20 (1994) 327–336.
[28] Ando Jumpei, Phase diagrams of $Ca_3(PO_4)_2$–$Mg_3(PO_4)_2$ and $Ca_3(PO_4)_2$–$CaNaPO_4$ systems, Bull. Chem. Soc. Jpn. 31 (1958) 201–205.
[29] J.X. Lu, M. Descamps, J. Dejou, G. Koubi, P. Hardouin, J. Lemaitre, J.P. Proust, The biodegradation mechanism of calcium phosphate biomaterials in bone, J. Biomed. Mater. Res. (Appl. Biomater.) 63 (4) (2002) 408–412.
[30] H.K. Koerten, J. van der Meulen, Degradation of calcium phosphate ceramics, J. Biomed. Mater. Res. 44 (1) (1999) 78–86.
[31] C.P.A.T. Klein, A.A. Driessen, K. de Groot, Biodegradation behavior of various calcium phosphate materials in bone tissue, J. Biomed. Mater. Res. 17 (5) (1983) 769–784.
[32] H.U. Cameron, I. MacNab, R.M. Pillar, Evaluation of a biodegradable ceramic, J. Biomed. Mater. Res. 11 (2) (1977) 179–185.
[33] S.N. Bhaskar, J.M. Brady, L. Getter, F. Grower, T. Driskell, Biodegradable ceramic implants in bone, Oral. Surg. 32 (2) (1971) 336–346.
[34] V. Sergey, A. Dorozhkin, Review on the dissolution models of calcium apatites, Prog. Cryst. Growth Charact. Mater. 44 (1) (2002) 45–61.
[35] M. Kohri, K. Miki, H. Waite, H. Nakajima, T. Okabe, In vitro stability of biphasic calcium phosphate ceramics, Biomaterials 14 (4) (1993) 299–304.
[36] S.R. Radin, P. Ducheyne, Effect of bioactive ceramic composition and structure on in vitro behaviour. III. Porous versus dense ceramics, J. Biomed. Mater. Res. 28 (11) (1994) 1303–1309.
[37] K. de Groot, in: P. Ducheyne, J. Lemons (Eds.), Bioceramics: Material Characteristics Versus In vivo Behaviour, Academy of Sciences, New York, 1988.
[38] R. Li, A.E. Clark, L.L. Hench, An investigation of bioactive glass powders by sol-gel processing, J. Appl. Biomater. 2 (4) (1991) 231–239.
[39] F.H. Kin, C.J. Liao, K.S. Chen, J.S. Sun, H.C. Liu, Degradation behavior of a new bioceramics: $Ca_2P_2O_7$ with addition of $Na_4P_2O_7{\cdot}10H_2O$, Biomaterials 18 (13) (1997) 915–921.
[40] W. Den Hollander, P. Patka, C.P. Klein, G.A. Heidendal, Macroporous calcium phosphate ceramics for bone substitution: a tracer study on biodegradation with ^{45}Ca tracer, Biomaterials 12 (6) (1991) 569–573.